Amyloid Fibrils of Glucagon Characterized by High-Resolution Atomic Force Microscopy

Kathy L. De Jong,* Bev Incledon,† Christopher M. Yip,‡ and Michael R. DeFelippis*
*Lilly Research Laboratories, Eli Lilly and Company, Indianapolis, Indiana; †Eli Lilly Canada, Toronto, Ontario, Canada; and ‡University of Toronto, Toronto, Ontario, Canada

ABSTRACT Glucagon solutions at pH 2.0 were subjected to mechanical agitation at 37°C in the presence of a hydrophobic surface to explore the details of aggregation and fiber formation. High-resolution intermittent-contact atomic force microscopy performed in solution revealed the presence of aggregates after 0.5 h; however, longer agitation times resulted in the formation of fibrillated structures with varying levels of higher-order assembly. Height, periodicity, and amplitude measurements of these structures allowed the identification of four distinct fiber types. The most elementary fiber form, designated a filament, self-associates in a specific wound fashion to produce protofibrils composed of two filaments. Subsequent self-assembly of these filaments and protofibrils leads to two well-defined fibrillar motifs, termed Type I and Type II. Atomic force microscopy imaging of pH 2.8 glucagon solutions not agitated or exposed to elevated temperature revealed the presence of amorphous aggregates before the formation of fibrillar structures similar to those seen at pH 2.0. Time-course solution Fourier transform infrared spectroscopy and thioflavin T binding studies suggested that glucagon aggregation and fibril formation were associated with the development of β-sheet structure. The results of these studies are used to describe a possible mechanism for glucagon aggregation and fibrillation that is consistent with a hierarchical assembly model proposed for amyloid fibril formation.

INTRODUCTION

The conversion of normally soluble proteins and peptides to insoluble fibrils or plaques referred to as amyloid is the subject of intense study, since the process has been associated with more than 20 different diseases (1–5). On a molecular basis, aggregation is driven by the existence of improperly folded structures; however, details concerning the mechanism of pathogenesis and the exact species involved are currently the subject of debate (5). Perhaps one of the more intriguing outcomes derived from research in this field is the understanding that nonnative self-assembly resulting in amyloid formation appears to be a generic property of polypeptide chains (2).

Nonnative self-assembly also presents one of the greatest challenges to the development of protein and peptide biopharmaceuticals (6,7). To maintain a therapeutic effect, the integrity of higher-order structural elements specific to a given molecule must be properly stabilized since disruptions to native conformation have the potential to promote aggregation, fibrillation, gelation, and/or precipitation that can lead to diminished activity or have serious toxicological, immunological, or pharmacological consequences (6,8,9). Many aspects related to formulation design of proteins and peptides have the potential to perturb native structure, including pH, ionic strength, concentration, or inclusion of excipients. In addition, environmental factors such as agitation, shear, pressure, interfaces, and temperature extremes encountered during manufacturing operations, distribution, storage, and handling of protein and peptide therapeutics can potentially compromise properly folded conformation.

A variety of strategies are available to address the problem of physical stabilization. For example, rational design to generate aggregation resistant analogs has proved to be feasible in certain cases but requires that amino acid changes do not impact activity or pharmacological properties (10). Addition of various formulation additives, although largely an empirical approach, has also been shown to be an effective way of stabilizing native structure or inhibiting aggregation (6,7). The more practical approach of minimizing or completely avoiding exposure to conditions that disrupt structure and/or promote aggregation is yet another option. However, to successfully apply any of these strategies to achieve the necessary physical stability for a protein or peptide biopharmaceutical product, a detailed understanding of structural properties and the factors that can potentially induce nonnative self-assembly is required.

Glucagon, a 29 amino acid peptide hormone playing an important endogenous role in maintaining normal circulating glucose levels, is commercially available as a pharmaceutical preparation for the treatment of hypoglycemia and other clinical applications (11). Due to limitations in both chemical and physical stability of glucagon, the pharmaceutical product is supplied as a lyophilized powder that must be used immediately after reconstitution with its supplied aqueous diluent (12). Of particular concern is the propensity of glucagon to aggregate resulting in the formation of fibrils and gels; a process that can be stimulated by acidic pH, increased

Submitted November 8, 2005, and accepted for publication May 31, 2006.

Address reprint requests to Michael R. DeFelippis, Biopharmaceutical Research and Development, Lilly Research Laboratories, Eli Lilly and Company, Drop Code 3844, Indianapolis, IN 46285. Tel.: 317-276-6027; Fax: 317-277-0833; E-mail: defelippis_michael_r@lilly.com.

Kathy L. De Jong's present address is Xerox Research Center Canada, Mississauga, Ontario, Canada.

0006-3495/06/09/1905/10 $2.00

doi: 10.1529/biophysj.105.077438

ionic strength, peptide concentration, agitation, and/or elevated temperatures (12,13). Therefore, glucagon provides an excellent relevant model for studying aggregation phenomena and approaches for stabilization that may be generally applicable to other protein and peptide biopharmaceuticals.

A recent report exploring the aggregation behavior of glucagon and other peptides has shown that aging glucagon solutions prepared at concentrations >2.5 mg/mL for 24 h results in the production of cytotoxic amyloidogenic fibrils (14). However, solutions prepared at the clinical concentration of 1 mg/mL only formed fibrils after aging for 30 days. The stabilizing effect afforded by the conditions used in the pharmaceutical preparation of glucagon is interesting and provides additional opportunities to explore other factors capable of inducing aggregation. In this work, we examine the mechanism of glucagon aggregation induced by agitation at elevated temperature in the presence of a hydrophobic surface. Structural features formed as a result of the physical stress conditions are characterized by high-resolution atomic force microscopy (AFM) and other biophysical techniques, including thioflavin T (ThT) fluorescence and solution-state Fourier transform infrared (FTIR) spectroscopy.

METHODS

Materials

Recombinant glucagon (98% purity as measured by reversed-phase high-performance liquid chromatography) was obtained from Eli Lilly and Company (Indianapolis, IN) and used without further purification. Sodium hydroxide and hydrochloric acid were purchased from Sigma (St. Louis, MO). ThT was purchased from MP Biomedicals (Aurora, OH). Ultrapure water (resistivity >18 MΩ cm) supplied from a Millipore (Bedford, MA) water purification system was used to prepare all solutions. Solid 1/8-inch diameter polytetrafluoroethylene (PTFE) beads used to provide a hydrophobic surface during mechanical agitation were obtained from Saint-Gobain Performance Plastics (Poestenkill, NY). Muscovite mica, the substrate used for AFM experiments, was purchased from SPI Supplies (West Chester, PA). D_2O, deuterated NaOH, and deuterated HCl were purchased from Sigma-Aldrich (Oakville, Ontario,Canada).

Initiation of glucagon aggregation

Glucagon solutions were prepared at a concentration of 1 mg/ml by first dissolving the peptide in 14 mM NaOH and stirring for 1.5 h. This base treatment step was conducted to remove any aggregated forms or fibril/gel seed nuclei that may be present in the glucagon used for the experiments (12). Liquid chromatography/mass spectrometry analysis conducted on base-treated glucagon solutions yielded molecular mass for the main peak and two most prominent isoforms that were in excellent agreement with the theoretical value for glucagon (3483 Da). We note that base treatment did not appear to affect aggregation or fiber formation compared to untreated solutions (data not shown). After the base treatment, the solutions were adjusted to either pH 2.0 or pH 2.8 using 1 N HCl and passed through Acrodisc (Pall, East Hills, NY) 0.2 μm low protein binding filters. Filtered solutions of glucagon were filled into 2 ml glass vials (Fisher Scientific, Hampton, NH) containing 10 PTFE beads to provide a hydrophobic surface of consistent surface area. Sufficient volume of the glucagon solution was added to avoid an air headspace, and the vial openings were covered with a 0.01'' PTFE liner and then sealed with a screw cap. Vials, PTFE beads and PTFE liners were soaked in 0.1 N HCl for 2 days, rinsed with ultrapure water until a constant pH was achieved, and thoroughly dried before use. To induce aggregation, the filled vials were attached horizontally to a New Brunswick Scientific model R2 reciprocal shaker (Edison, NJ), housed in a laboratory oven, and agitated (100 rpm) at a controlled temperature of 37°C for various lengths of time.

AFM imaging

Intermittent-contact (tapping-mode) AFM imaging was performed in fluid using a Digital Instruments NanoScope III Multimode Atomic Force Microscope (Veeco/Digital Instruments, Santa Barbara, CA) equipped with an ''E'' scanner (13.6 μm × 13.6 μm maximum lateral scan area) using 100 μm oxide-sharpened silicon nitride V-shaped cantilevers with a nominal spring constant of ~0.32 N/m installed in a combination contact/tapping mode liquid flow-cell sealed against a freshly cleaved mica substrate. All images were collected as 512 × 512 pixel data sets at a typical scan rate of 1–2 Hz with a vertical tip oscillation frequency of 7–9 KHz. The AFM samples were prepared by direct deposition of an 8 μl aliquot of the glucagon solutions onto freshly cleaved mica. All imaging was performed in fluid using protein-free solution. Fibril height, amplitude, and periodicity data were obtained using the Nanoscope software section analysis tool and quoted as the mean of 30–50 measurements ± SD.

Infrared spectroscopy

Glucagon samples were prepared at a concentration of 1 mg/ml in 14 mM deuterated NaOH with stirring for 1.5 h, followed by adjusting the pH to 2.0 or 2.8 using 1 N DCl. Solutions were then passed through Acrodisc (Pall) 0.2 μm low protein binding filters. The pH 2.0 solutions were filled into 2 ml glass vials (Fisher Scientific) containing 10 PTFE beads and agitated for 2 h as previously described. FTIR spectra were acquired with a Nicolet 6700 spectrometer equipped with a Thermo (Waltham, MA) Spectra-Tech Micro Circle Cell Mount and a ZnSe rod, controlled by OMNIC software version 7.2. Single beam spectra were collected at a resolution of 2 cm^{-1} from 4000 to 400 cm^{-1}. Spectra were processed using the OMNIC software package. Final spectra represent averages of 500 scans after buffer subtraction, followed by water vapor subtraction to remove excessive noise.

Thioflavin T-binding

Vials containing glucagon solutions were subjected to mechanical agitation at 37°C in the presence of a hydrophobic surface (PTFE beads, as described earlier). At various times, vials were removed from the reciprocal shaker and a 720 μl of sample was transferred to a 1.5 ml Eppendorf (Hamburg, Germany) tube. An 80 μl aliquot of ThT solution prepared in water adjusted to pH 2.0 was added to the glucagon sample to achieve a final concentration of 30 μM of the fluorescent probe. Black, untreated microtiter plate wells (Nalge Nunc International, Rochester, NY) were filled with 150 μl of the glucagon containing ThT solutions. Fluorescence intensity was monitored over time at ambient temperature using a SpectraMax GeminiEM Fluorescence Microtiter Plate Reader (Molecular Devices, Sunnyvale, CA) with excitation and emission wavelengths of 440 nm and 480 nm, respectively. Samples were measured at ambient, rather than elevated (37°C), temperatures to arrest the aggregation process at specific time points.

RESULTS AND DISCUSSION

The pharmaceutical preparation of glucagon is a lyophilized powder reconstituted to a concentration of 1 mg/ml with an aqueous pH 2.0 diluent. Under these clinically relevant conditions, glucagon is physically stable when used as instructed.

In a recent study evaluating the aggregation propensity of glucagon, 1 mg/ml solutions in 0.01 M HCl showed no formation of amyloidogenic fibers unless stored for longer periods of time (14). These investigators also demonstrated that other factors such as glucagon concentration and temperature accelerated fibrillation; however, specific mechanistic and molecular details concerning the nature of the process were not provided. To address these questions concerning glucagon aggregation and fibrillation, we employed in situ intermittent-contact AFM, a scanning probe technique that operates by measuring repulsive and attractive forces between a vertically oscillating tip and the sample of interest (15).

Whereas glucagon aggregation and fibril formation is notably slower at pH 2.0, the process can be accelerated by mechanical agitation at elevated temperature enabling investigation of the assembly process into higher-order structures within a 24 h time period. To achieve rapid and reproducible aggregation under controlled conditions, we adapted the experimental system previously described to study the nonnative assembly mechanism of insulin resulting from exposure to a hydrophobic interface (16). After shaking at 37°C in the presence of a hydrophobic surface provided by the addition of PTFE beads, glucagon solutions appeared clear with no apparent change in viscosity detected by visual examination, irrespective of the duration of agitation. Inspection of pH 2.0 glucagon solutions by AFM after agitation for 0.5 h revealed aggregates that were loosely bound to the mica substrate (Fig. 1 *a*). In contrast, AFM analysis of glucagon solutions agitated for 5 or 20 h revealed fibrillar structures (Fig. 1, *b* and *c*). Close inspection of these structures revealed a well-defined axial periodicity (Fig. 1 *b*). These mature fibers are primarily unbranched and were up to several microns long. Morphologically, these glucagon fibers appeared very similar to the amyloid fibrils formed by a variety of other proteins including Aβ-amyloid (17), α-synuclein (18), and Ig light-chain protein SMA (19) (SMA are the initials of the patient whose sequence was used to clone the gene coding for the variable domain of lg light chain). At longer agitation times, individual glucagon fibers appeared to wind together to yield higher-order structures, and, in some cases, gave the appearance of branching, as seen in the center of Fig. 1 *b*. The interaction of individual fibers, which may represent stages of the winding process, can be seen in Fig. 1 *c* (*arrows* at *left* of image). At the region noted by arrow 1, two fibers lie parallel and are ''in phase''. The fibers are ''out of phase'' in the region indicated by arrow 2, and appear to wind together to form a single feature having periodicity noted by arrow 3. A perspective view of these features is shown in Fig. 1 *d*.

Since feature width determinations are strongly dependent on the size and shape of the AFM tip (20), height

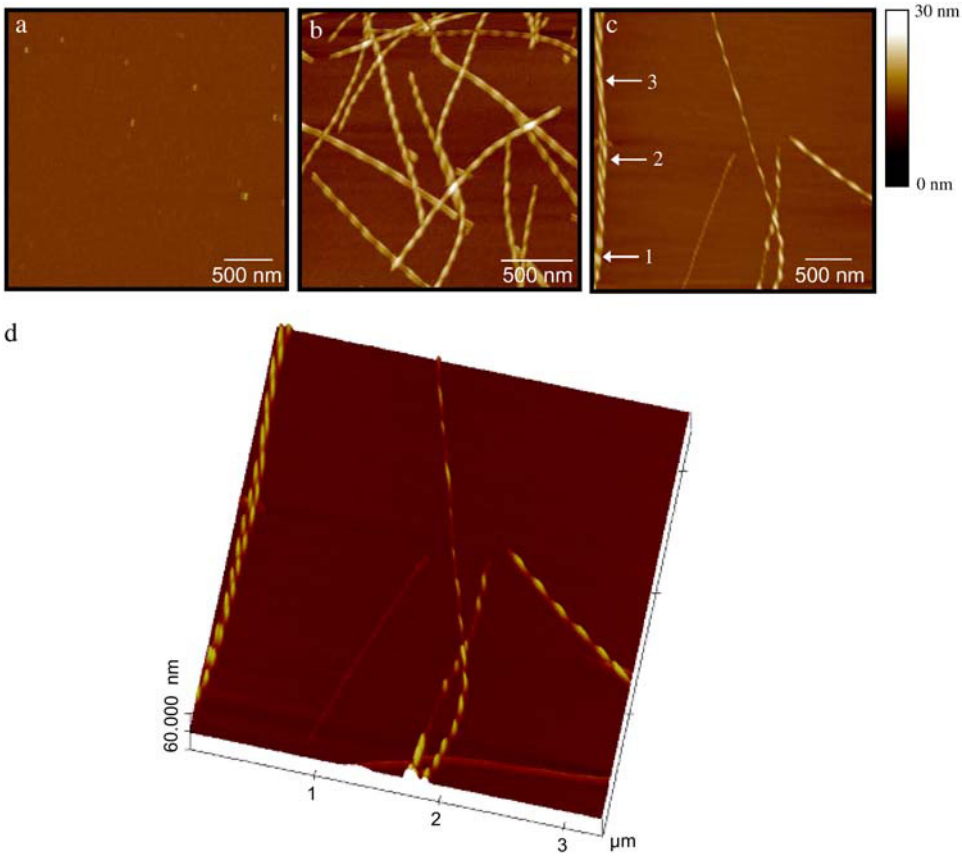

FIGURE 1 (*a*) AFM height image of a 1 mg/ml pH 2.0 glucagon solution agitated at 37°C in the presence of a hydrophobic surface for 0.5 h. (*b*) After continued agitation for 5 h, fibers are observed with periodicity along the fibril length. (*c*) Individual fibers can be resolved ''in phase'' and ''out phase'' (*numbered white arrows*; see text for additional details) in the twisting process and with varied thickness after agitation for 20 h. (*d*) Perspective view of panel (*c*). Vertical scale bar shows height gradation with progression from darker to lighter color corresponding to taller features.

measurements were used to characterize the different glucagon fiber structures that formed during agitation. Height measurements were performed at two positions along a single fiber shown in Fig. 2 *a*. A fiber height of 2.4 ± 0.2 nm was obtained from an analysis of multiple cross sections perpendicular to the portion of the fiber labeled *F*. Further along the same fiber, the height in the area labeled *P* is 4.7 ± 0.3 nm, nearly twice the previous measurement. The region that is 2.4 ± 0.2 nm is the smallest height measurement observed in the analysis of multiple AFM images of glucagon solutions agitated longer than 0.5 h. We introduce the term filament to describe fibers having this height. In our model, the region of the fiber that is nearly twice the original filament height results from the interaction of a second filament with the first to yield, upon winding, a putatively periodic structural feature. A similar winding of individual filaments has been observed during amyloid formation of the Ig light-chain protein SMA (19). These investigators used the term protofibril to describe the structure that results from the assembly of two filaments, and we use this same nomenclature here to describe glucagon fibers having a height of ~4.0 nm. Two additional distinct fiber morphologies are observed in Fig. 2 *b*. The fiber indicated with the label *TI* has a height of 9.0 ± 0.6 nm, a value twice that of a protofibril. This measurement suggests the assembly of two protofibrils that have wound together to form the fiber. A structure with this height was also identified in aggregated Ig light-chain protein SMA and designated a Type I fibril (19). Height measurements of the fiber identified with the label *TII* in Fig. 2 *b* revealed a value of 7.0 ± 0.5 nm, suggesting the assembly of three filaments wound together. Amyloid fibers of Ig light-chain protein SMA with this same morphology have been termed Type II fibrils (19). The highly ordered Type I and Type II glucagon fibrils as shown in Fig. 2 *b* were typically observed with extended agitation times. It is important to note that we cannot discount the possibility of alternate assembly pathways giving rise to these same Type I and Type II fibril motifs. These include the association of a filament with a protofibril to yield a Type II fibril, a protofibril with two filaments to form a Type I fibril, or a filament with a Type II fibril resulting in a Type I fibril (see Fig. 7).

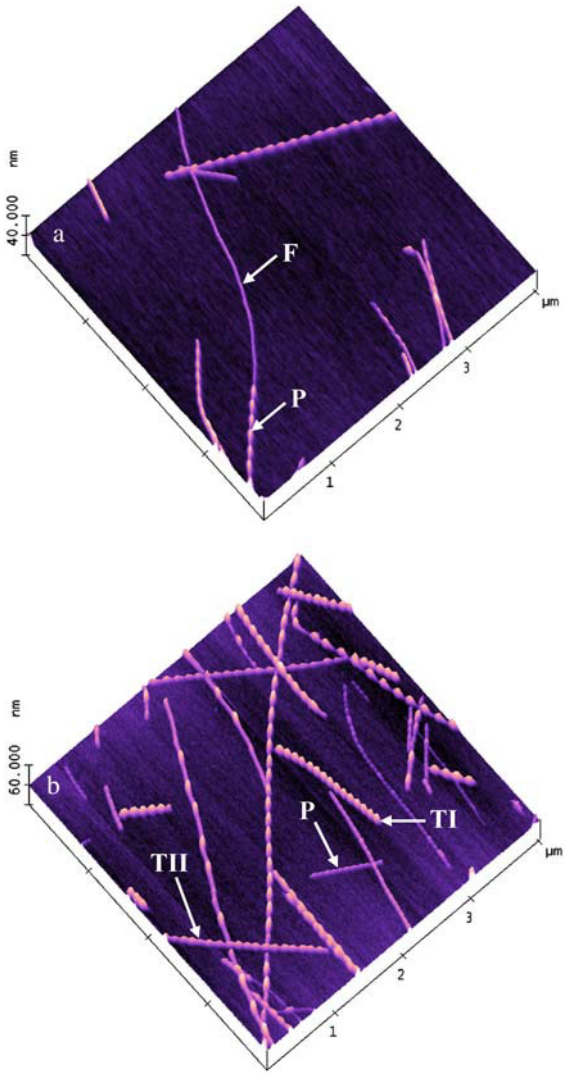

FIGURE 2 (*a*) AFM height images corresponding to a filament (labeled *F*) and protofibril (labeled *P*) formed after 4 h of agitation at 37°C in the presence of a hydrophobic surface. (*b*) AFM height images corresponding to a Type I (labeled *TI*) fibril, Type II (labeled *TII*) fibril, and protofibril (labeled *P*) formed after 5 h of agitation using the same conditions as described in panel *a*. Height measurements on the fibers in panel *a* were obtained by section analysis yielding mean ± SD values of 2.4 ± 0.2 nm ($n = 15$) and 4.7 ± 0.3 nm ($n = 8$) for the filament and protofibril, respectively. Similar height analyses performed on the fibers shown in panel *b* yielded mean ± SD values of 9.0 ± 0.6 nm ($n = 14$) and 7.0 ± 0.5 nm ($n = 16$) for the Type I and Type II fibrils, respectively.

Amplitude and periodicity measurements on the various glucagon fiber forms are made by profiling the structures parallel to the long axis as shown in Fig. 3, *a–c*. Amplitudes are measured by averaging height differences between each peak and trough of the twist (*red arrowheads*). The amplitude should be approximately equal to, or less than, the height of individual filaments or protofibrils forming the wound structure. Amplitudes for the Type I and Type II fibrils shown in Fig. 3 are in good agreement with the heights of individual protofibrils and filaments comprising these fiber types (Fig. 2). In contrast, the amplitude for the protofibril is approximately half the height of a single filament. Periodicities are determined by averaging the peak to peak distance of the twist (*green arrowheads*). These measurements are indicative of how the individual filaments or protofibrils are twisted together to form the various fiber types.

Height, amplitude, and periodicity measurements determined from AFM images of aggregated glucagon are in close agreement with those obtained for amyloid fibers of the Ig light-chain protein SMA, despite substantial differences in protein amino acid composition (Table 1) (19). Indeed,

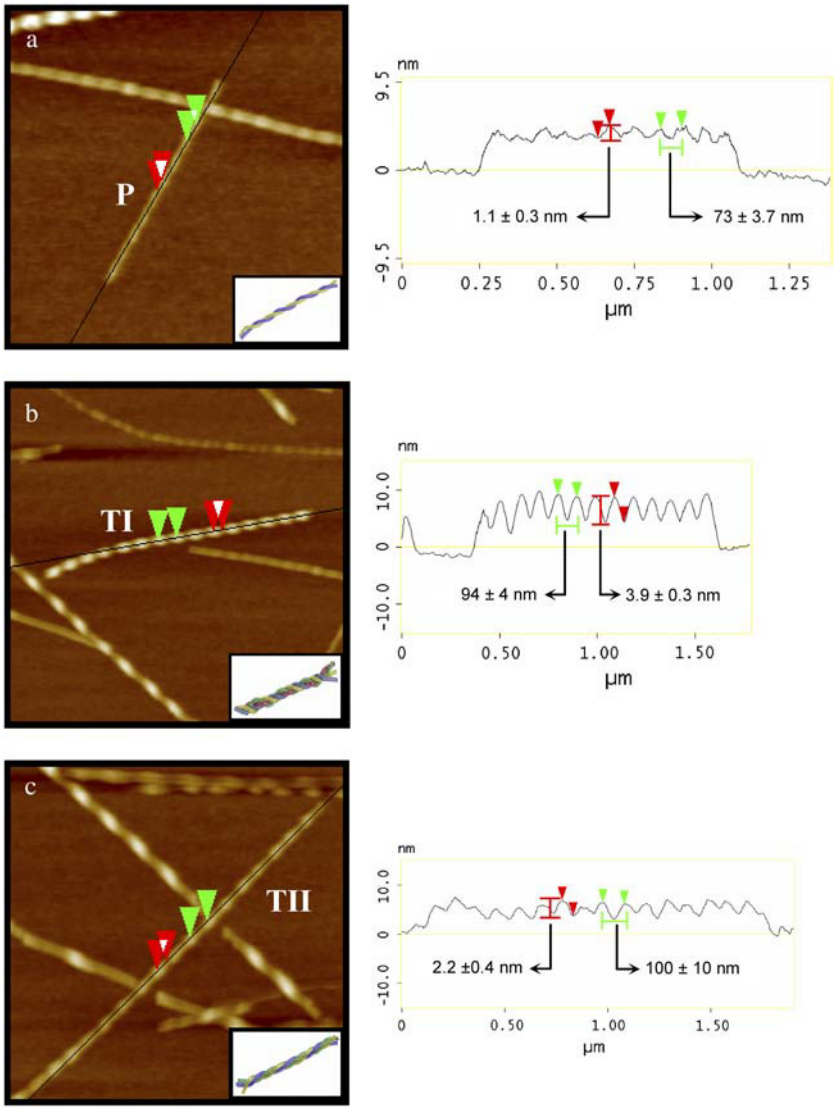

FIGURE 3 By profiling a fiber parallel to its long axis, amplitude and periodicity measurements were obtained for (*a*, *P*) protofibril, (*b*, *TI*) Type I fibril, and (*c*, *TII*) Type II fibril. Mean ± SD values are indicated for amplitude (*red arrowheads*) and periodicity (*green arrowheads*) measurements. The number of amplitude and periodicity measurements determined for individual fiber types shown in panel *a* is 10 and 9; panel *b* is 12 and 12; and panel *c* is 14 and 17. Insets show representations of fiber winding motifs.

recent AFM studies have shown that amyloid fibers obtained from molecularly and functionally diverse proteins are structurally similar (17,18,19,21,22). Although filament formation may be influenced by amino acid sequence, for instance through cysteine-mediated disufide bond formation, it has been recently suggested that long-range quaternary structure interactions may facilitate amyloid fiber formation (23). Regardless of how the filaments and/or fibers form, when structural comparisons are made between amyloid fibers, differences in the experimental conditions during imaging must be taken into consideration. In Table 1, the dimensions reported for fibers produced in agitated glucagon solutions are for hydrated structures, and it is not unexpected that these measurements are marginally higher in some instances than those of the dried Ig light-chain protein SMA (19). We further note that Type II fibril periodicity and amplitude data for the Ig light-chain protein SMA fibers were not reported. Recent x-ray diffraction and electron microscopy data collected on a variety of amyloid forming proteins have suggested that these fiber structures are water-filled nanotubes (24). In the case of Ig light-chain protein SMA, dehydration may cause the fibers to collapse thereby influencing height, periodicity and amplitude measurements. It is therefore important when comparing structural characteristics and motifs between proteins, that the AFM imaging conditions be self-consistent (i.e., either in air or similarly hydrated).

The formation of mature glucagon fibrils is consistent with the general hierarchical assembly model for amyloid fibers proposed by Khurana et al. (18). However, the conditions employed to generate glucagon fibers made it difficult to capture early events in the assembly process before the appearance of fibrous structures. We have observed considerable numbers of all fiber species (e.g., filaments, protofibrils, Type I, and Type II fibrils) within 4–5 h after agitation at 37°C in the presence of a hydrophobic surface. Without any

TABLE 1 AFM measurements obtained for glucagon aggregated structures

Structure	Measurement	Glucagon*	Ig light-chain†
Filament	Height	2.4 ± 0.3	2.4 ± 0.5
Protofibril	Height	3.9 ± 0.7 nm	4.0 ± 0.6 nm
	Periodicity	67 ± 8 nm	60 ± 10 nm
	Amplitude	1.1 ± 0.3 nm	0.8 ± 0.4 nm
Type I fibril	Height	9.0 ± 0.8 nm	8.3 ± 1.0 nm
	Periodicity	93 ± 7.2 nm	100 ± 10 nm
	Amplitude	4.1 ± 0.7 nm	1.6 ± 0.3 nm
Type II fibril	Height	6.8 ± 0.7 nm	5.9 ± 0.6 nm
	Periodicity	115 ± 25 nm	–
	Amplitude	3.1 ± 1.2 nm	–

*Values stated for glucagon fibrils are mean ± SD obtained from 30–50 height, periodicity, and amplitude measurements for each fibril type from three different images.
†Results from Ionescu-Zanetti et al. (19) shown for comparison.

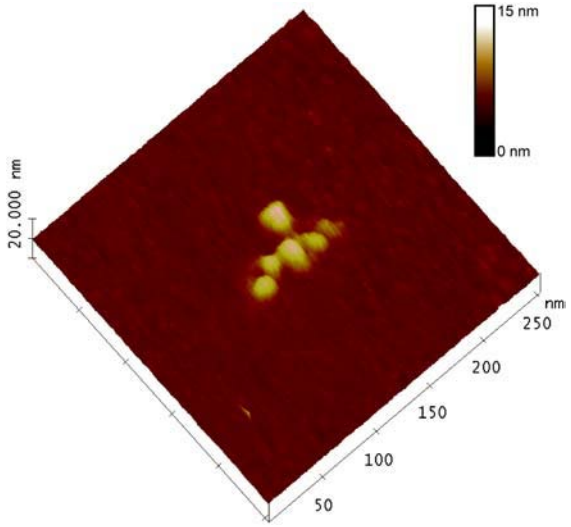

FIGURE 4 AFM height image obtained for a 1 mg/ml pH 2.8 glucagon solution aged 6 h at ambient temperature. The large amorphous aggregate remained adsorbed to the mica over multiple scans. Vertical scale bar shows height gradation with progression from darker to lighter color corresponding to taller features.

stimulus, glucagon solutions at pH 2.0 are quite stable and not prone to aggregation or fibril growth unless left for extended periods of time (i.e., days to months). The work of Onoue et al. confirmed the pH 2.0 stabilization effect for glucagon (14). In contrast, glucagon solutions prepared at pH 2.8 show a marked increase in the rate of fibril formation compared to pH 2.0, and physical stress imparted by agitation, elevated temperature, or exposure to a hydrophobic surface is not necessary to initiate the fibrillation process. Fibers formed at pH 2.8 show similar morphology to those produced at pH 2.0 (data not shown). In an attempt to determine whether other structural features occur before the formation of filaments and/or protofibrils, in situ AFM was employed to examine 1 mg/ml solutions of glucagon at pH 2.8.

AFM images obtained on the pH 2.8 glucagon solutions immediately after preparation show structural features representative of aggregated peptide randomly distributed over the mica surface similar to those shown in Fig. 1 *a*, but the aggregates are easily dislodged with scanning even under low imaging forces. Upon aging of the solution (i.e., hours), stable imaging of larger aggregates was achieved (Fig. 4). At its maximum height, the structural feature observed is 4.4 nm and is taller than a single filament formed after agitation at elevated temperature in the presence of a hydrophobic surface (Table 1). Similar clusters of amorphous particles were observed in AFM images obtained on acidic solutions of insulin exposed to elevated temperatures for 30–60 s, and it was proposed that these entities were involved in the fibril assembly process (21). Loosely packed amorphous structures were also observed in AFM images obtained for Ig light-chain protein SMA solutions prepared at higher pH conditions than pH 2.0 where fibrils are readily produced (25). Both fibrils and amorphous deposits form in Ig light-chain protein SMA solutions after extended storage over days. Such aggregate intermediates may retain higher water content resulting in a more bulky appearance than mature fibrils since the release of water is expected to be characteristic of fibril formation (26–28).

Although we were unable to directly visualize the transformation of the amorphous aggregates into fibers for the pH 2.8 glucagon solutions, we contend that these structures represent nascent prefibrillar precursors since the predominant features observed by AFM after 24 h of incubation are filaments and higher-order fiber types. It should be noted that our interpretations are based on imaging of surface-bound species and that we cannot account for transformations that occur in the bulk solution phase. Drying of samples before AFM imaging, as was done in other work (21), can stop the process at various times, enabling better resolution of the apparent time-dependent relationship between the various structural forms, but one needs to be concerned about the possibility of inducing features as a result of water removal. Care must also be exercised in the interpretation of our AFM data collected under different aggregation/fiber forming conditions. Other work has shown that the mechanism of fibril formation for the Ig light-chain protein SMA on surfaces was significantly different than in solution (29). In studies on $A\beta_{1-40}$, solid-state ^{13}C NMR was capable of resolving different fibril morphologies depending on whether they were formed under quiescent conditions or with agitation (30). Within the resolution capabilities of the atomic force microscope, it does not appear that the different conditions used to generate glucagon fibrils in our work influences the mechanism of growth.

The conformational properties of proteins and peptides in solution are important factors since partially folded states are thought to be critical intermediates involved in aggregation and subsequent fibril formation (25,31,32,33,34). Glucagon is a small, flexible peptide that can adopt a variety of conformational forms depending on solution conditions

(35–38). The x-ray crystal structure indicates that the hormone adopts a mainly α-helical structure, but this result is likely influenced by the conditions used to prepare crystals (39). Far-UV circular dichroism (CD) spectroscopy was used to determine the conformation of glucagon at the pH conditions used in our studies (data not shown). Whereas the CD spectrum of a nonagitated glucagon solution at pH 2.0 revealed a predominantly random coil conformation with some β-sheet character, we were unable to obtain CD spectra on agitated glucagon solutions due to optical artifacts presumably resulting from the presence of aggregated forms in the samples. We further note that CD spectroscopy revealed no structural change for 1 mg/ml pH 2.0 glucagon solutions that had been stored quiescently for 24 h. To further explore solution state conformational properties of glucagon, time-course FTIR spectroscopy was performed on 1.0 mg/mL glucagon solutions adjusted to pH 2.0 and agitated at 37°C for 2 h in the presence of a hydrophobic surface. After this treatment, we observed a spectral feature at $\sim$1620 cm^{-1} that developed over a 24-h period consistent with the transformation of glucagon to a β-sheet structure (Fig. 5). Glucagon solutions prepared at pH 2.8 but not agitated nor exposed to 37°C produced a similar spectral change over the same time period (data not shown). These features are consistent with those reported for air-dried glucagon fibrils examined by attenuated total reflection-FTIR spectroscopy (40).

To complement our CD and FTIR data and noting that stacking of β-sheets is the predominant structure postulated for fibers, a dye binding assay using the extrinsic fluorescent probe ThT was applied to study the glucagon fibrillation process. This approach is commonly used to demonstrate the existence of β-sheets within the amyloid fibers (41,42). ThT is quenched in solution, but binding to β-sheet structures provides the correct environment for interactions that result in fluorescence enhancement (43). A characteristic fluorescence emission response consists of a lag period, followed by a growth phase that eventually plateaus at a constant value (32). Increases in dye binding and subsequent fluorescence intensity responses have been correlated with the growth of fibrils (19,32). Fluorescence emission was monitored in a series of glucagon solutions adjusted to pH 2.0 and agitated for 2, 5, and 20 h at 37°C in the presence of a hydrophobic surface. Immediately after agitation, ThT was added and fluorescence intensities were monitored over 24 h. Dye binding events are observed for all samples (Fig. 6), with the longest agitation time exhibiting the highest initial fluorescence emission signal. Note that the typical fluorescence emission profile is not obtained, presumably because the lag period is over after 2 h of agitation and the fibrillation process is in full progress. The increasing fluorescence intensity observed over time for samples agitated 2 and 5 h indicates that glucagon fibrils

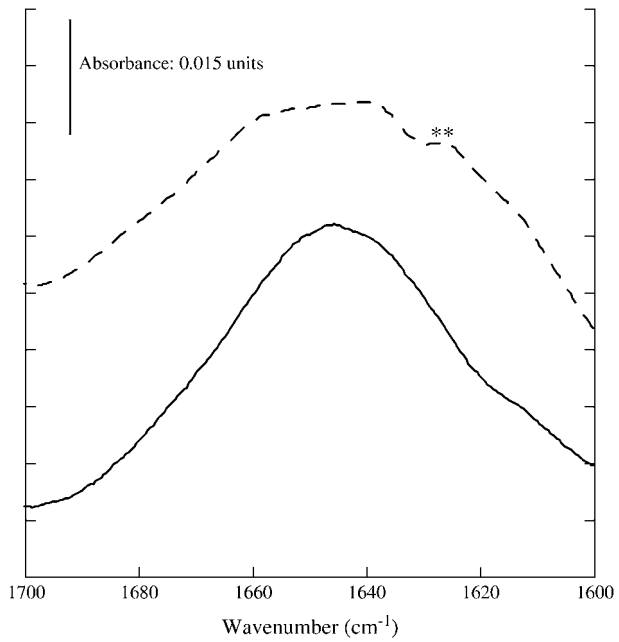

FIGURE 5 FTIR spectra for 1 mg/ml pH 2.0 glucagon acquired in deuterated buffer solution for (*a*) $t = 0$ (*solid line*) and (*b*) $t = 22.5$ h (*dashed line*) after agitation for 2 h at 37°C in the presence of PTFE beads. Spectra are plotted on a common absorbance scale and are vertically offset for clarity. (**) Spectral band at $\sim$1620 cm^{-1}.

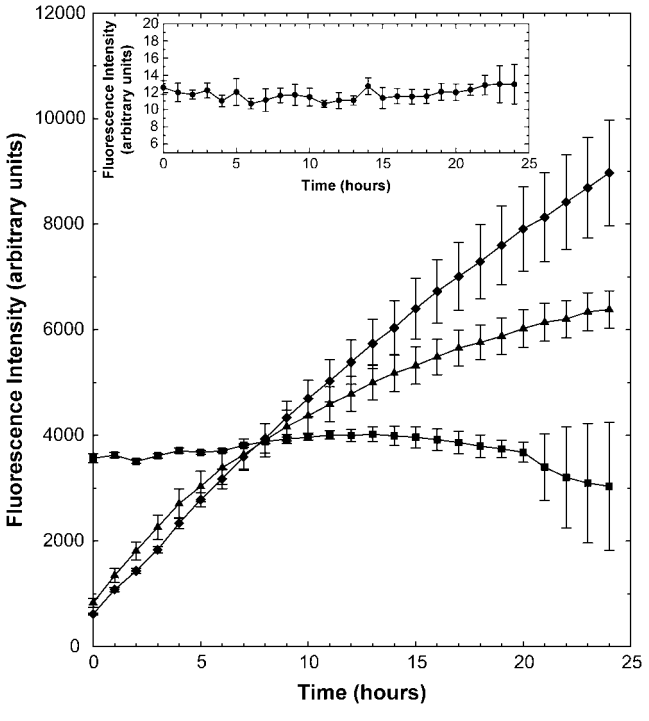

FIGURE 6 ThT fluorescence was monitored in a series of 1 mg/ml pH 2.0 glucagon samples agitated at 37°C in the presence of a hydrophobic surface for 2 h (♦), 5 h (▲). or 20 h (■). After agitation at the indicated times, an aliquot of each sample was removed and mixed with ThT. Fluorescence emission was monitored at 480 nm. (*Inset*) ThT fluorescence from control sample not exposed to agitation or elevated temperature (●). Data represents mean ± SD for four replicates.

continue to bind ThT during the time period after agitation. In contrast, the sample agitated for 20 h remains relatively constant throughout the observation period with an endpoint fluorescence lower than that of samples agitated 2 and 5 h. This result argues that ThT cannot access the interior of tightly wound glucagon fibrils formed (i.e., after 20 h of agitation) before the addition of ThT (Fig. 1 *c*) and further suggests completion of the fibrillation process. In the absence of agitation (i.e., $t = 0$ h on stock solution), we did not observe any evidence of fluorescence enhancement (Fig. 6, *inset*). Although these fluorescence and FTIR experiments strongly suggest that fiber formation in glucagon is associated with the development of β-sheet structure, it should be noted that ThT fluorescence is not a conclusive marker of β-sheet structure, as has been reported recently (40), and that the observed ThT fluorescence is a consequence of a number of factors, including fibril density and filament orientation.

Taken collectively, the results of our studies suggest a potential mechanism for glucagon aggregation/fibrillation. Our fluorescence dye binding and time-course FTIR spectroscopy data indicate that a conformational transition occurs resulting in an increased level of β-sheet structure that may initiate aggregation. Although structural changes and partially folded intermediates have been implicated as critical precursors in the aggregation/fibrillation mechanisms of other proteins (25,31–34,44), we cannot dismiss the possibility that glucagon may be inherently poised to aggregate without requiring a conformational change to stimulate self-assembly, and that the observed increase in β-sheet structure is a consequence of intermonomer interactions. Inspection of the amino acid sequence reveals a contiguous stretch of β-sheet favoring residues at positions 22–27 that may predispose glucagon toward aggregation (45). Despite this uncertainty in the initiation events, it appears that aggregates (Figs. 1 *a* and 4) are produced early in the fibrillation process and these forms may serve as the nucleus for filament growth. As the fibrillation process progresses over time, the filaments self-assemble and twist together to produce protofibrils, as well as Type I and Type II fibrils

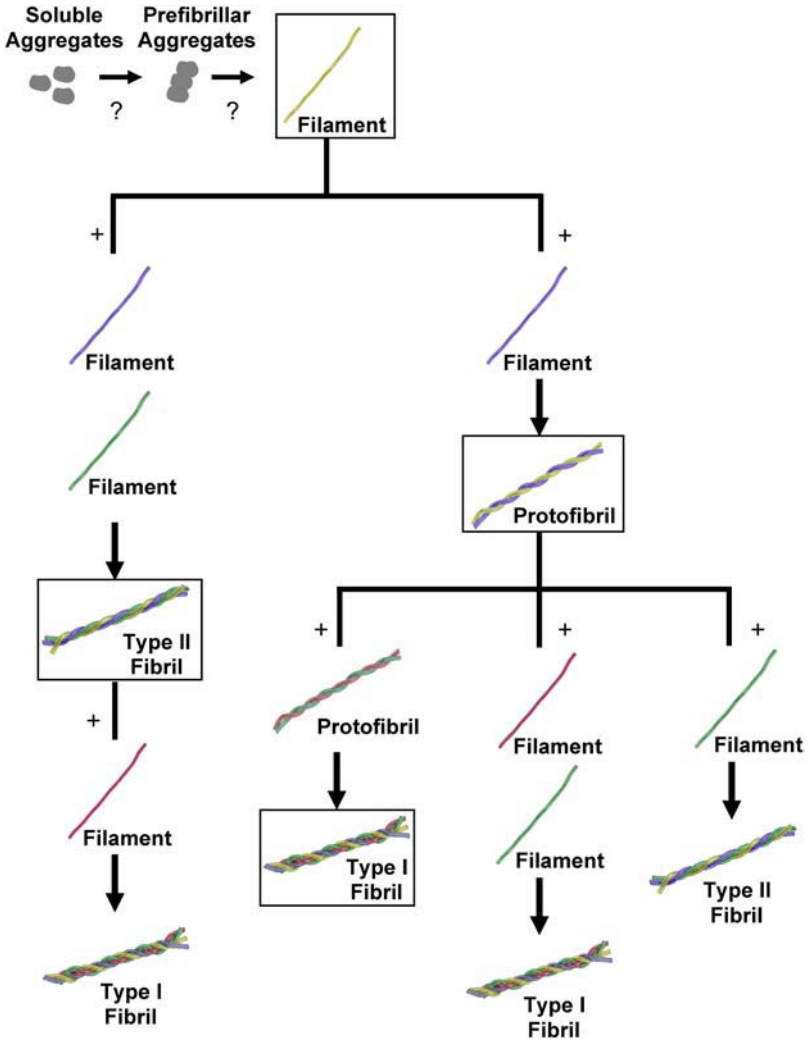

FIGURE 7 Glucagon aggregation and fibrillation process. Under appropriate conditions, glucagon self-associates, leading to the formation of soluble aggregates and agglomerated forms that may be prefibrillar structures. These putative prefibrillar precursors may grow into filaments that self-assemble to produce protofibrils, Type I and Type II fibrils, by a variety of assembly mechanisms.

(Fig. 7). Further work is required to elucidate the exact mechanistic details of the fibrillation pathway for glucagon.

Our AFM studies have enabled the characterization of structural details involved in the glucagon aggregation/fibrillation process. Although a recent study on glucagon has demonstrated that the peptide can aggregate to produce cytotoxic amyloidogenic fibrils, high-resolution information on the nature of the fibrous material was not provided (14). We have determined the molecular properties of glucagon fibrils to be remarkably consistent with those demonstrated for other amyloidogenic proteins and peptides (2–5), and further suggest a putative mechanism for their formation that is consistent with a general hierarchical model proposed for amyloid assembly based on reported AFM studies (18).

Glucagon offers a distinct advantage over other proteins/peptides for studying the mechanism of amyloid formation because solution conditions under which aggregation/fibrillation occurs are relevant to the pharmaceutical preparation and its clinical use. A common practice in this field is to employ atypical solution conditions and grossly elevated temperatures to instigate aggregation and fibrillation. For example, insulin fibrils are formed in highly acidic pH solutions exposed to temperatures of 60°C or more for extended periods of time (21,46). Pharmaceutical preparations of insulin typically do not experience these extreme conditions, leaving some uncertainty about the practical relevance of such studies. Furthermore, acidic pH and high temperature are known to accelerate chemical degradation of insulin and other proteins/peptides in general (47). The implications of such complex mixtures of various native and chemically degraded forms of insulin on the mechanism of aggregation and fibrillation remain poorly understood. Glucagon, however, allows for examination of its aggregation and fibrillation mechanisms under pharmaceutically relevant acidic pH solution conditions within a time period where chemical degradation is less of an issue.

Stabilization of natively folded protein and peptide structures against conformational denaturation, aggregation, and potential fibrillation is a considerable challenge and generally hinders the development and commercialization of biopharmaceutical products (6,7). These degradation pathways must be prevented or adequately controlled because the resulting end products can have diminished activity and/or serious toxicological, immunological, or pharmacological consequences (6,8,9). Current approaches used for stabilization, however, are mostly empirical (6,7). A detailed molecular understanding of degradation pathways involving higher-order structural transitions, as demonstrated here for glucagon, will ultimately enable more rational design of physically stable biopharmaceutical formulations.

The common mechanistic features emerging for nonnative protein/peptide assembly have additional important implications for amyloid deposition diseases. Despite significant diversity in amino acid sequences and three-dimensional folding, a number of proteins and peptides have been shown to produce highly similar fibrillated structures (2,3,4,5,48). Understanding details of the aggregation/fibrillation mechanism at the molecular level is crucial to developing approaches for pharmaceutical treatment or possible prevention of amyloid deposition diseases. Glucagon can also serve as an ideal model system for such studies.

The authors thank Kelly McAllister, Sarah Demmon, Lisa Coelho, and David Marquardt of Eli Lilly and Company for assistance with fluorescence, FTIR, and liquid chromatography/mass spectrometry measurements. Muppalla Sukumar of Eli Lilly and Company is thanked for helpful discussions and assistance with collecting the circular dichroism data.

Kathy L. De Jong was the recipient of a Lilly Research Laboratories Postdoctoral Fellowship.

REFERENCES

1. Sipe, J. D. 1992. Amyloidosis. *Annu. Rev. Biochem.* 61:947–975.
2. Dobson, C. M. 1999. Protein misfolding, evolution and disease. *Trends Biochem. Sci.* 24:329–332.
3. Dobson, C. M. 2001. The structural basis of protein folding and its links with human disease. *Philos. Trans. R. Soc. Lond. B Biol. Sci.* 356: 133–145.
4. Dobson, C. M. 2004. Principles of protein folding, misfolding and aggregation. *Semin. Cell Dev. Biol.* 15:3–16.
5. Stefani, M., and C. M. Dobson. 2003. Protein aggregation and aggregate toxicity: new insights into protein folding, misfolding diseases and biological evolution. *J. Mol. Med.* 81:678–699.
6. Frokjaer, S., and D. E. Otzen. 2005. Protein drug stability: a formulation challenge. *Nat. Rev. Drug Discov.* 4:298–306.
7. Wang, W. 2005. Protein aggregation and its inhibition in biopharmaceutics. *Int. J. Pharm.* 289:1–30.
8. Cleland, J. L., M. F. Powell, and S. J. Shire. 1993. The development of stable protein formulations: a close look at protein aggregation, deamidation, and oxidation. *Crit. Rev. Ther. Drug Carrier Syst.* 10: 307–377.
9. Schellekens, H. 2002. Bioequivalence and the immunogenicity of biopharmaceuticals. *Nat. Rev. Drug Discov.* 1:457–462.
10. Fowler, S. B., S. Poon, R. Muff, F. Chiti, C. M. Dobson, and J. Zurdo. 2005. Rational design of aggregation-resistant bioactive peptides: reengineering human calcitonin. *Proc. Natl. Acad. Sci. USA.* 102: 10105–10110.
11. Hall-Boyer, K., G. P. Zaloga, and B. Chernow. 1984. Glucagon: hormone or therapeutic agent? *Crit. Care Med.* 12:584–589.
12. Bromer, W. W. 1983. Chemical characteristics of glucagon. *In* Glucagon. I. P. J. Lefèbvre, editor. Springer-Verlag, Berlin Heidelberg. 1–22.
13. Beaven, G. H., W. B. Gratzer, and H. G. Davies. 1969. Formation and structure of gels and fibrils from glucagon. *Eur. J. Biochem.* 11:37–42.
14. Onoue, S., K. Ohshima, K. Debari, K. Koh, S. Shioda, S. Iwasa, K. Kashimoto, and T. Yajima. 2004. Mishandling of the therapeutic peptide glucagon generates cytotoxic amyloidogenic fibrils. *Pharm. Res.* 21:1274–1283.
15. Binnig, G., C. F. Quate, and Ch. Gerber. 1986. Atomic force microscope. *Phys. Rev. Lett.* 56:930–933.
16. Sluzky, V., J. A. Tamada, A. M. Klibanov, and R. Langer. 1991. Kinetics of insulin aggregation in aqueous solutions upon agitation in the presence of hydrophobic surfaces. *Proc. Natl. Acad. Sci. USA.* 88: 9377–9381.
17. Harper, J. D., S. S. Wong, C. M. Lieber, and P. T. Lansbury Jr. 1999. Assembly of Aβ amyloid protofibrils: an in vitro model for a possible early event in Alzheimer's disease. *Biochemistry.* 38:8972–8980.

18. Khurana, R., C. Ionescu-Zanetti, M. Pope, J. Li, L. Nielson, M. Ramirez-Alvarado, L. Regan, A. L. Fink, and S. A. Carter. 2003. A general model for amyloid fibril assembly based on morphological studies using atomic force microscopy. *Biophys. J.* 85:1135–1144.

19. Ionescu-Zanetti, C., R. Khurana, J. R. Gillespie, J. S. Petrick, L. C. Trabachino, L. J. Minert, S. A. Carter, and A. L. Fink. 1999. Monitoring the assembly of Ig light-chain amyloid fibrils by atomic force microscopy. *Proc. Natl. Acad. Sci. USA.* 96:13175–13179.

20. Wong, S. S., J. D. Harper, P. T. Lansbury, Jr., and C. M. Lieber. 1998. Carbon nanotube tips: high-resolution probes for imaging biological systems. *J. Am. Chem. Soc.* 120:603–604.

21. Jansen, R., W. Dzwolak, and R. Winter. 2005. Amyloidogenic self-assembly of insulin aggregates probed by high resolution atomic force microscopy. *Biophys. J.* 88:1344–1353.

22. Goldsbury, C., J. Kistler, U. Aebi, T. Arvinte, and G. J. S. Cooper. 1999. Watching amyloid fibrils grow by time-lapse atomic force microscopy. *J. Mol. Biol.* 285:33–39.

23. Jiménez, J. L., E. J. Nettleton, M. Bouchard, C. V. Robinson, C. M. Dobson, and H. R. Saibil. 2002. The protofilament structure of insulin amyloid fibrils. *Proc. Natl. Acad. Sci. USA.* 99:9196–9201.

24. Perutz, M. F., J. T. Finch, J. Berriman, and A. Lesk. 2002. Amyloid fibers are water-filled nanotubes. *Proc. Natl. Acad. Sci. USA.* 99:5591–5595.

25. Khurana, R., J. R. Gillespie, A. Talapatra, L. J. Minert, C. Ionescu-Zanetti, I. Millett, and A. L. Fink. 2001. Partially folded intermediates as critical precursors of light chain amyloid fibrils and amorphous aggregates. *Biochemistry.* 40:3525–3535.

26. Balbirnie, M., R. Grothe, and D. S. Eisenberg. 2001. An amyloid-forming peptide from the yeast prion Sup35 reveals a dehydrated beta-sheet structure for amyloid. *Proc. Natl. Acad. Sci. USA.* 98:2375–2380.

27. Dzwolak, W., R. Ravindra, J. Lendermann, and R. Winter. 2003. Aggregation of bovine insulin probed by DSC/PPC calorimetry and FTIR spectroscopy. *Biochemistry.* 42:11347–11355.

28. Lipfert, J., J. Franklin, F. Wu, and S. Doniach. 2005. Protein misfolding and amyloid formation for the peptide GNNQQNY from yeast prion protein Sup35: simulation by reaction path annealing. *J. Mol. Biol.* 349:648–658.

29. Zhu, M., P. O. Souillac, C. Ionescu-Zanetti, S. A. Carter, and A. L. Fink. 2002. Surface-catalyzed amyloid fibril formation. *J. Biol. Chem.* 277:50914–50922.

30. Petkova, A. T., R. D. Leapman, Z. Guo, W. M. Yau, M. P. Mattson, and R. Tycko. 2005. Self-propagating, molecular-level polymorphism in Alzheimer's β-amyloid fibrils. *Science.* 307:262–265.

31. Nielsen, L., S. Frokjaer, J. Brange, V. N. Uversky, and A. L. Fink. 2001. Probing the mechanism of insulin fibril formation with insulin mutants. *Biochemistry.* 40:8397–8409.

32. Nielsen, L., R. Khurana, A. Coats, S. Frokjaer, J. Brange, S. Vyas, V. N. Uversky, and A. L. Fink. 2001. Effect of environmental factors on the kinetics of insulin fibril formation: elucidation of the molecular mechanism. *Biochemistry.* 40:6036–6046.

33. Ahmad, A., I. S. Millett, S. Doniach, V. N. Uversky, and A. L. Fink. 2003. Partially folded intermediates in insulin fibrillation. *Biochemistry.* 42:11404–11416.

34. Kirkitadze, M. D., M. M. Condron, and D. B. Teplow. 2001. Identification and characterization of key kinetic intermediates in amyloid [beta]-protein fibrillogenesis. *J. Mol. Biol.* 312:1103–1119.

35. Gratzer, W. B., E. Bailey, and G. H. Beaven. 1967. Conformational states of glucagon. *Biochem. Biophys. Res. Commun.* 28:914–919.

36. Gratzer, W. B., G. H. Beaven, H. W. E. Rattle, and E. M. Bradbury. 1968. A conformational study of glucagon. *Eur. J. Biochem.* 3:276–283.

37. Gratzer, W. B., and G. H. Beaven. 1969. Relation between conformation and association state. A study of the association equilibrium of glucagon. *J. Biol. Chem.* 244:6675–6679.

38. Wagman, M. E., C. M. Dobson, and M. Karplus. 1980. Proton NMR studies of the association and folding of glucagon in solution. *FEBS Lett.* 119:265–270.

39. Sasaki, K., S. Dockerill, D. A. Adamiak, I. J. Tickle, and T. Blundell. 1975. X-ray analysis of glucagon and its relationship to receptor binding. *Nature.* 257:751–757.

40. Pedersen, J. S., D. Dikov, J. L. Flink, H. A. Hjuler, G. Christiansen, and D. E. Otzen. 2006. The changing face of glucagon fibrillation: structural polymorphism and conformational imprinting. *J. Mol. Biol.* 355:501–523.

41. Naiki, H., K. Higuchi, M. Hosokawa, and T. Takeda. 1989. Fluorometric determination of amyloid fibrils in vitro using the fluorescent dye, thioflavin T1. *Anal. Biochem.* 177:244–249.

42. Ban, T., M. Hoshino, S. Takahashi, D. Hamada, K. Hasegawa, H. Naiki, and Y. Goto. 2004. Direct observation of a beta amyloid fibril growth and inhibition. *J. Mol. Biol.* 344:757–767.

43. Krebs, M. R., E. H. Bromley, and A. M. Donald. 2005. The binding of thioflavin-T to amyloid fibrils: localisation and implications. *J. Struct. Biol.* 149:30–37.

44. Bouchard, M., J. Zurdo, E. J. Nettleton, C. M. Dobson, and C. V. Robinson. 2000. Formation of insulin amyloid fibrils followed by FTIR simultaneously with CD and electron microscopy. *Protein Sci.* 9:1960–1967.

45. Chou, P. Y., and G. D. Fasman. 1974. Prediction of protein conformation. *Biochemistry.* 13:222–245.

46. Brange, J., L. Andersen, E. D. Laursen, G. Meyn, and E. Rasmussen. 1997. Toward understanding insulin fibrillation. *J. Pharm. Sci.* 86:517–525.

47. Brange, J. 1992. Chemical stability of insulin. 4. Mechanisms and kinetics of chemical transformations in pharmaceutical formulation. *Acta Pharm. Nord.* 4:209–222.

48. Sunde, M., L. C. Serpell, M. Bartlam, P. E. Fraser, M. B. Pepys, and C. C. Blake. 1997. Common core structure of amyloid fibrils by synchrotron X-ray diffraction. *J. Mol. Biol.* 273:729–739.